DeepLC can predict retention times for peptides that carry as-yet unseen modifications

Robbin Bouwmeester[†,‡], Ralf Gabriels[†,‡], Niels Hulstaert[†,‡], Lennart Martens[†,‡,§], and Sven Degroeve[†,‡]

†VIB-UGent Center for Medical Biotechnology, VIB, Ghent, Belgium
‡Department of Biomolecular Medicine, Ghent University, Ghent, Belgium

§ To whom correspondence should be addressed
Tel: +32 9 224 98 40
Email: lennart.martens@vib-ugent.be
Address: Technologiepark Zwijnaarde 75, 9052 Gent, Belgium

ORCID IDs:
Robbin Bouwmeester: https://orcid.org/0000-0001-6807-7029
Ralf Gabriels: https://orcid.org/0000-0002-1679-1711
Niels Hulstaert: https://orcid.org/0000-0003-1172-5202
Lennart Martens: https://orcid.org/0000-0003-4277-658X
Sven Degroeve: https://orcid.org/0000-0001-8349-3370

Abstract

The inclusion of peptide retention time prediction promises to remove peptide identification ambiguity in complex LC-MS identification workflows. However, due to the way peptides are encoded in current prediction models, accurate retention times cannot be predicted for modified peptides. This is especially problematic for fledgling open modification searches, which will benefit from accurate retention time prediction for modified peptides to reduce identification ambiguity. We here therefore present DeepLC, a novel deep learning peptide retention time predictor utilizing a new peptide encoding based on atomic composition that allows the retention time of (previously unseen) modified peptides to be predicted accurately. We show that DeepLC performs similarly to current state-of-the-art approaches for unmodified peptides, and, more importantly, accurately predicts retention times for modifications not seen during training. Moreover, we show that DeepLC's ability to predict retention times for any modification enables potentially incorrect identifications to be flagged in an open modification search of CD8-positive T-cell proteome data. DeepLC is available under the permissive Apache 2.0 open source license and comes with a user-friendly graphical user interface, as well as a Python package on PyPI, Bioconda, and BioContainers for effortless workflow integration.

Introduction

Liquid Chromatography (LC) plays a critical role in Mass Spectrometry (MS) analysis of bottom-up proteomics[1]. By separating peptides based on their physicochemical properties in the LC step, the complexity of the sample presented to the MS instrument is greatly reduced. This reduction means that there is less ionization competition, improved sensitivity for data dependent/independent analysis, and reduced chimericity in fragmentation spectra (MS^2) [2,3]. In addition to these benefits, the retention time measurement itself provides an additional dimension of information to interpret the signals generated by a peptide[4]. In order to interpret these acquired signals, they need to be matched with earlier observations of the same peptides or with a prediction of the signal.

However, the process by which a peptide is retained or eluted is not fully understood yet[5], which means that libraries with previously observed retention times are often used to match to newly acquired signals[6]. However, these libraries are often incomplete and moreover are non-transferable between experimental setups without calibration. In order to fill this knowledge gap, researchers have therefore used models to predict retention times for previously unobserved peptides[4].

Many of the first methods for peptide retention time prediction relied on simulation models based on physicochemical knowledge[7]. However, most modern approaches use data-driven methods such as machine learning (ML) or deep learning (DL) algorithms to train a predictive model[8–12]. In such models, the mapping between the peptide sequence (or features derived from this sequence)

57 and the LC retention time apex is learned from empirical examples. After training, these models
58 can be used to generate predictions for unobserved peptides.

59 Such retention time prediction models have already been successfully applied for various tasks in
60 proteomics analysis workflows, e.g. to improve identification confidence[13,14], to design more
61 efficient experiments[15], and to identify chimeric fragmentation spectra[16]. Most recently, these
62 retention time prediction models have been used in combination with fragment peak intensity
63 prediction models to generate comprehensive, *in silico* chromatogram libraries for Data
64 Independent Acquisition (DIA) identification, effectively replacing and surpassing more limited,
65 empirically derived Data Dependent Acquisition (DDA) spectral libraries[17–19].

66 In keeping with the general trend in ML, there has been a switch from classical ML to DL in newly
67 developed retention time predictors. This switch was mainly driven by recent innovations in the
68 field of DL and the large amount of peptide retention time data that has become available. The
69 types of architectures proposed by state-of-the-art DL retention time models include capsule
70 convolutional neural networks (CNNs) in DeepRT(+)[11], NN with long short-term memory (LSTM)
71 layers as used by Guan et al.[9], and an encoder-decoder principle with gated recurrent units (GRU)
72 in Prosit[10]. The architectures of these models either work with a CNN or recurrent architecture
73 (e.g. LSTM or GRU units). CNN architectures slide a filter with a specified kernel size over the
74 encoded peptide. In contrast, recurrent neural networks thread the sequence through a sequence
75 of units.

76 However, all these models share the same peptide encoding method, in which amino acids and
77 their corresponding positions are transformed into a one-hot amino acid encoding. This encoding

takes the form of a matrix in which the presence or absence of each amino acid for each position in the peptide is represented by a one or a zero, respectively.

Unfortunately, this use of one-hot encoding of amino acids restricts the models' applicability in some of the most interesting data analysis workflows, most notably in open modification searches (OMS), where the goal is to elucidate the modification landscape of the proteome[20–23]. These OMS workflows are gaining popularity in the field of proteomics as they make it possible to search for a large variety of peptide modifications simultaneously.

Unfortunately, current retention time prediction methods cannot be directly applied in OMS because of the vast amount of potential modifications[24]. With one-hot amino acid encoding, each potential modification needs to be represented by a binary feature indicating the presence of this modification. Additionally, sufficient training examples are required for each modification for the ML algorithm to learn the hidden impact of every one of these modifications on the peptide retention time.

We here solve this fundamental issue with DeepLC, our novel retention time predictor that is able to accurately predict the retention time for all peptides and their modifications, even when these modifications have not been seen during training. DeepLC achieves this by encoding peptides and modifications at the atomic composition level, allowing generalization of the patterns learned from the modifications seen during training.

Results

The results section is split in two main parts. We first evaluate the performance of DeepLC on retention time prediction for unmodified peptides, in comparison with state-of-the-art tools. We then proceed to evaluate DeepLC on retention time prediction for modified peptides, which is an ability that is unique to DeepLC. We therefore rely on two distinct ways of evaluating DeepLC's performance on these modified peptides: (i) evaluate DeepLC performance on unseen modifications, and (ii) a novel type of evaluation which leaves out unmodified amino acids, and then has DeepLC treat these as modified glycines. These evaluations show that DeepLC is not only competitive with state-of-the-art retention time prediction algorithms for unmodified peptides, but can also achieve similar performance for unseen modified peptides. Finally, we illustrate a practical use of this unique capability by showing DeepLC's ability to flag false positive identifications in the results of an open modification search of a CD8-positive T-cell data set.

Evaluation of DeepLC against the state-of-the-art on unmodified peptides

Our approach to model amino acids by their atomic composition provides accurate predictions of LC retention times for unmodified peptides, with similar performance to current state-of-the-art retention time prediction models DeepRT[11], Prosit[10], and Guan et al.[9] that model amino acids directly. Note that the definition used here for "unmodified" can include the two very common artefactual modifications of carbamidomethylation of cysteine and oxidation of methionine.

DeepLC test set predictions for the three selected data sets are plotted in Figure 1. We observe very high prediction accuracy, with Pearson correlations larger than 0.99 for two of the data sets, and with the *HeLa HF* data set showing slightly worse performance (Pearson=0.984). For the latter,

117 the LC gradient is significantly shorter than for the other two data sets, implying that retention
118 times become less predictable, thus resulting in a slightly less performant model. Figure 1 also
119 reveals a small but significant number of peptides with high prediction errors that do not follow
120 the main trend. These are potentially wrong identifications or wrongly determined elution apexes.
121 The same plots for the other seventeen data sets can be found in Supplementary Figures 1 and 2
122 where we make very similar observations to those in Figure 1.

123 Supplementary Table 1 summarizes the test set performance for all twenty data sets described in
124 the data sets & evaluation section of the methods. The atomic composition encoding approach
125 of DeepLC is able to learn accurate prediction models with high R values for all data sets. For most
126 data sets DeepLC achieves an R above 0.98, with four data sets even achieving correlations above
127 0.995. This R value is highly comparable to the other models. Nearly all data sets were obtained
128 with reverse phase columns, yet even though there are fewer data sets with HILIC and SCX, DeepLC
129 also performs very well on these data sets with relative MAE errors below 1.5 %.

130 For the $\Delta t_{95\%}$ metric the differences are somewhat more pronounced. Here we observe that
131 DeepLC performs consistently worse than the other models. It is however unclear whether these
132 differences should be accounted to the atomic composition encoding, a different DL architecture,
133 a difference in train-validation-test split (note that for the other prediction models the manuscript
134 did not mention the use of a validation set), or a combination of these. As we want to focus on
135 the capability of DeepLC to predict retention times for modified peptides we leave this question
136 open for further research.

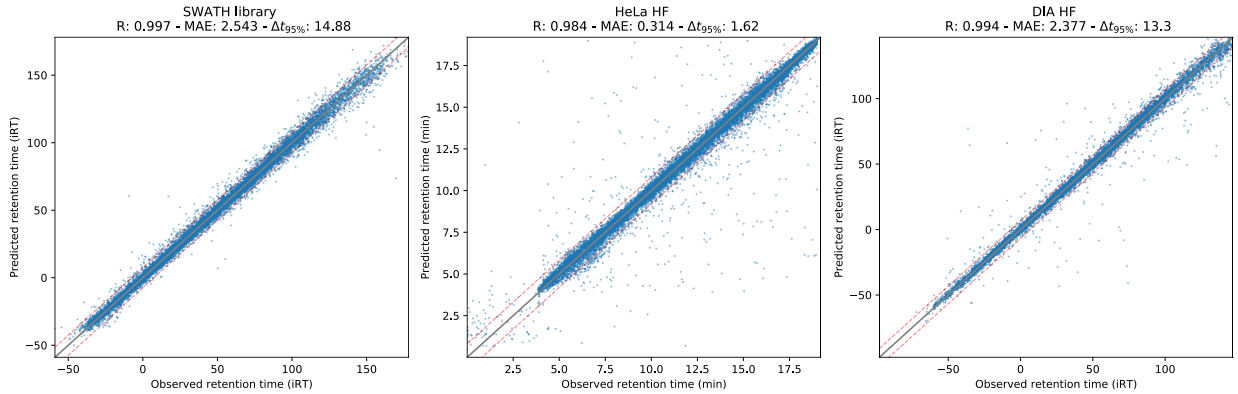

Figure 1: Scatter plot of predicted against observed on three of the largest data sets; *SWATH Library*, *HeLa HF*, and *DIA HF*.

The trained models are also highly transferrable between different data sets. This transferability is especially useful when applying models trained on larger data sets to smaller ones and application of the models without retraining. Only a simple calibration is required to transfer the predictions between LC setups. Supplementary Figure 3 shows that models that achieve high performance on a given data set also show high Spearman correlation when applied to different data sets.

DeepLC builds on a DL approach that greatly benefits from a large number of training peptides, and we can show that large data sets indeed do have a positive influence on the performance of DeepLC. The performance on each individual data set in relation to the number of training peptides is shown in Figure 2 and Supplementary Table 1. Data sets with a very small number of training peptides (< 10 000) tend to have a performance between 2 % and 4.5 % relative MAE. For medium sized data sets (> 10 000 and < 75 000 peptides), the performance can vary widely, with relative MAE's ranging from 0.9 % to 4.5 %. For larger data sets (> 75 000 peptides) the performance tends to be below 2 % relative MAE.

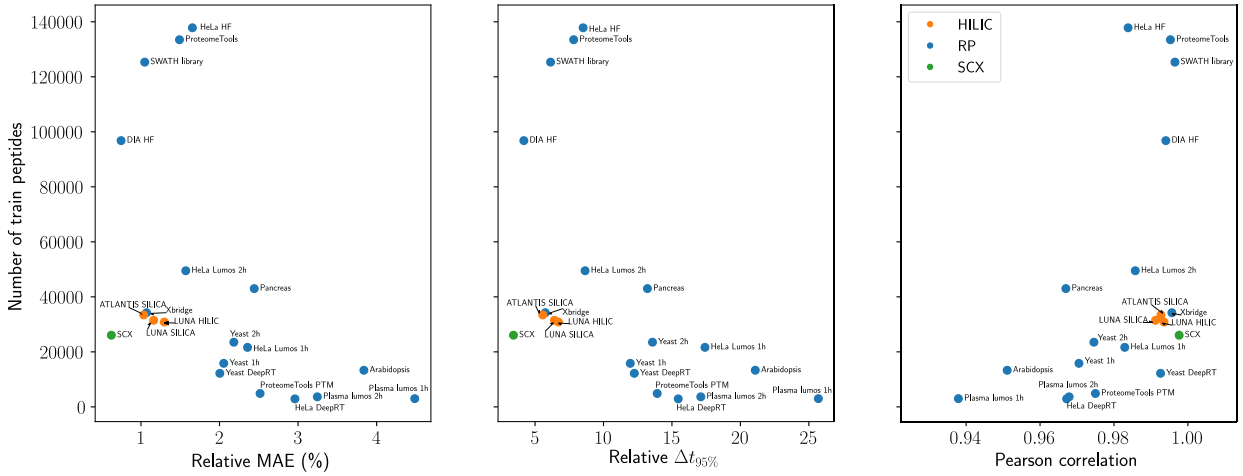

Figure 2: For the twenty data sets the number of training peptides (y-axis) is plotted against the relative MAE (left), relative $\Delta t_{95\%}$ (middle) and Pearson correlation (right).

To further evaluate the relationship between the number of training peptides and prediction performance we computed learning curves for the three selected data sets (Figure 3). For each data set, learning curve evaluation was performed five times with different test set subsamples. These curves show a sharp improvement for the first four to five steps (comprising up to 50 percent of the total number of training peptides). Beyond these steps, prediction performance improves only linearly for the *SWATH library* and *HeLa HF*, while showing smaller improvements in the last step for *DIA HF*. Importantly, for two of these data sets the performance continues to improve right to the last step of the learning curve. This ability to continuously improve performance suggests that DeepLC, like most other DL approaches, is capable of fitting even more complex relations than classical ML when provided with sufficient data. The same observation of increasing performance for larger training sets can be made for the remaining seventeen data sets (Supplementary Figures 4 and 5), with fifteen data sets showing clear improvement for the last two steps of the learning curve.

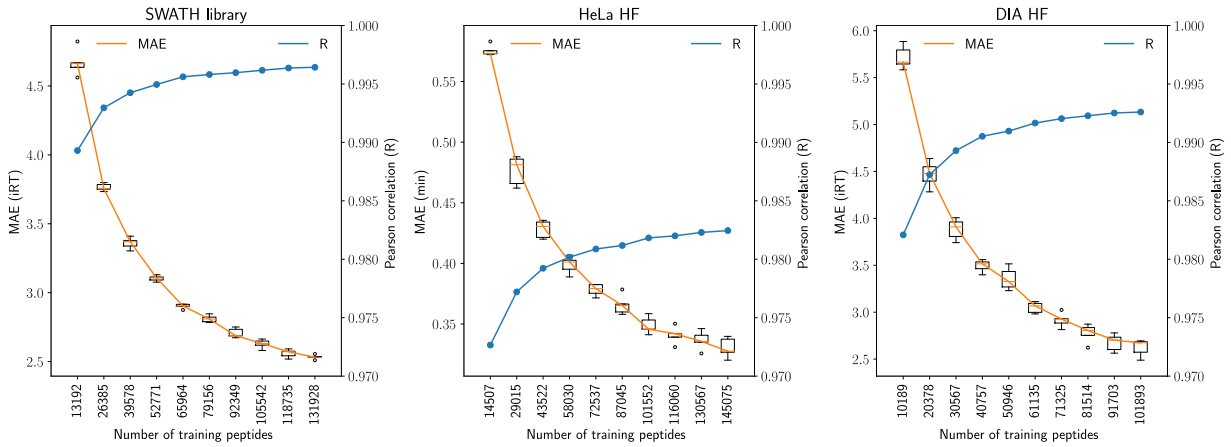

Figure 3: Learning curves for each of the three selected data sets. Prediction performances (R and MAE) for models trained on different training set sizes (x-axis) are computed for a fixed test set.

Performance evaluation for modified peptides

DeepLC is able to generalize effectively for unmodified peptides as well as extending its accurate retention time predictions to modifications that were not included in the training set. We can thus show that the DeepLC models have not just learned the general shift in retention time caused by modifications, but also how this shift depends on the context of the modification in the peptide. These claims are supported by two separate evaluations in this section.

Prediction performance for modified peptides would ideally be evaluated on a large data set with a variety of modifications. Indeed, as shown in Figure 3, the full performance potential of DeepLC is achieved by the largest possible data set size. However, such large data sets with many modifications are currently not available in the public domain.

Instead, we here show DeepLC's prediction performance for modified peptides on a recently published smaller data set (*ProteomeTools PTM*[25]), after the custom preprocessing workflow described in the methods section, comprising fourteen different modifications with known

185 location in 4099 synthetic peptides. Furthermore, we introduce an evaluation procedure that
186 allows the use of larger data sets based on the fact that any amino acid (apart from glycine) can
187 be considered as a modified glycine.

188 We first evaluate DeepLC on all fourteen modifications in the *ProteomeTools PTM* data set. We
189 trained and optimized fourteen DeepLC models, where each model only sees peptides that don't
190 contain a specific modification *M*. Each model is named after the modification it was not provided
191 with, so model *M* is trained and optimized only on those peptides that do not contain modification
192 *M*. Each model is then evaluated on the remaining peptides, which all do contain the modification
193 *M* that was excluded during training. We created two test sets from these remaining peptides to
194 evaluate predictions: one where the excluded modification is encoded and one where it is not.
195 Prediction performance for both test sets were then evaluated and compared. This comparison
196 thus allows performance to be assessed on a modification that is not included in training, in terms
197 of the improvement that DeepLC offers over a baseline of simply ignoring the presence of the
198 modification.

199 Figures 4 and Supplementary Figure 6 show the prediction errors for each of the left-out
200 modifications for training. In Figure 4, the boxplots show performance when a given modification
201 was not present in the training set for the model, and is afterwards either not encoded (red
202 boxplots; baseline) or encoded (blue boxplots) during the predictions. It should be noted that
203 many modifications did not cause a substantial change in terms of predicted retention time, as
204 was also observed in the original paper for this data set[25] Examples of such modifications with
205 limited impact are methyl, dimethyl, trimethyl, and deamidation. In contrast, the acyl modifications

206 (including propionyl, succinyl, malonyl, crotonyl, and acetyl) show a clear performance increase
207 when these modifications are encoded during the predictions. For instance, Supplementary Figure
208 6 shows that the MAE is improved by 700% (from 462 s to 66 s) for propionyl. These improvements
209 are mainly due to the correct prediction by DeepLC of the shift in retention time caused by the
210 modification, despite DeepLC never having encountered that specific modification before. Most
211 importantly, besides a significantly decreased MAE, the correlation R also shows a substantial
212 improvement. This is shown in Figure 4 through the substantially smaller variance for the blue box
213 plots. For crotonyl, for instance, Supplementary Figure 6 presents an increase of R from 0.975 to
214 0.990 when encoding the modification in the test set. This means that the DeepLC models have
215 not just learned the general shift in retention time caused by modifications, but also how this shift
216 depends on the context of the modification in the peptide.

217 Only nitrotyrosine and phosphorylation modifications show lower performance when encoded,
218 but these modifications can be classified as physicochemically very different from the other
219 modifications. This inability of DeepLC to accurately predict retention times for modifications that
220 are chemically very different from anything encountered the training set indicates that even
221 DeepLC requires some relevant training data for a given class of modifications.

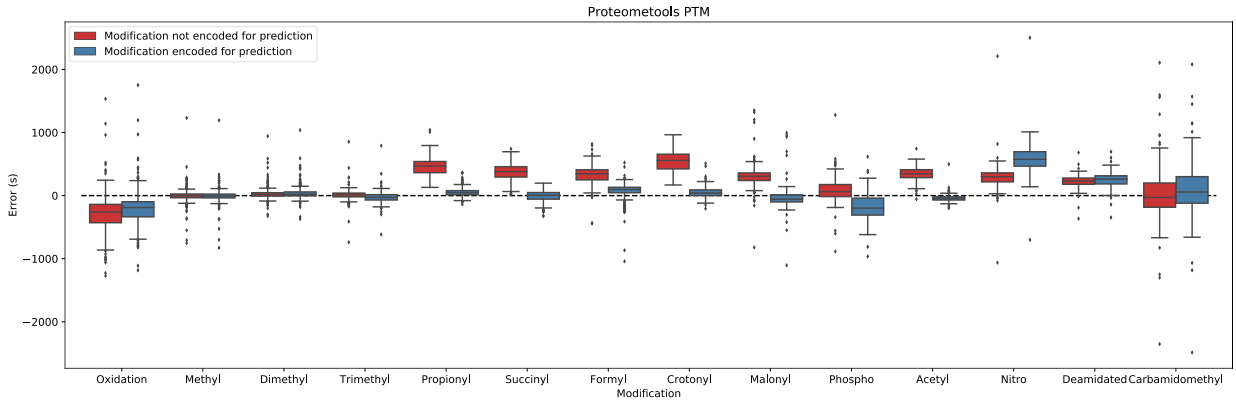

Figure 4: The modification that was excluded for training is shown on the horizontal axis, and the vertical axis shows the retention time error (experimental - predicted) when the modification was either not encoded (red) or encoded during the predictions (blue).

In the second evaluation procedure we used the larger *DIA HF* and the smaller *HeLa HF* data sets to train and optimize nineteen DeepLC models, where each model only sees peptides that do not contain a specific amino acid. The nomenclature is as above, in which model A is trained and optimized only on peptides that do not contain amino acid A. Next, each model is evaluated on all those peptides that do contain the excluded amino acid not seen during training. For this we again created two test sets from these remaining peptides: one where the excluded amino acid is encoded as the composition of glycine only and one with its actual composition.

We show that encoding an amino acid as itself instead of as glycine improves the MAE for most amino acids (Figure 5). DeepLC performs very well when modelling large hydrophobic residues as modified glycines, and slightly less well when modelling polar uncharged and negatively charged residues as modified glycines. Finally, for the positively charged amino acids only arginine shows an improvement, while lysine and histidine decrease in performance when encoding the amino acid. The poor performance for lysine can be explained by the difference with the amino acid with the closest atomic composition. For lysine the closest atomic compositions are arginine and

240 leucine (or isoleucine), which are significantly less hydrophobic or more hydrophobic, respectively.
241 This is similar to our observations for modifications, where the best performance is obtained for
242 unseen modifications which can be more readily extrapolated from already seen modifications.

243 Between the larger and smaller data sets there is a consistent performance difference between
244 the excluded amino acids. This consistency means that the observations made are likely to be
245 independent of the specific data set the evaluation is run on.

246 This non-modified amino acid evaluation shows that performance is slightly worse in comparison
247 to including the amino acid in the training set, with *DIA HF and HeLa DeepRT* having a MAE of
248 2.37 and 3.2 minutes, respectively. The MAE errors shown in Figure 5 are about 1.5 to 2.5 times
249 higher.

250 It is important to note that this evaluation is not only hard because the trained model has never
251 seen a given amino acid, it is also hard because peptides that are similar to each other are likely
252 to all be excluded from training due to these peptides having a higher likelihood of also containing
253 the removed amino acids. This can create biased training sets, especially for lysine and arginine
254 as the majority of peptides are tryptic. Surprisingly, however, the model is still able to predict
255 retention times very accurately for amino acids that were not used in training.

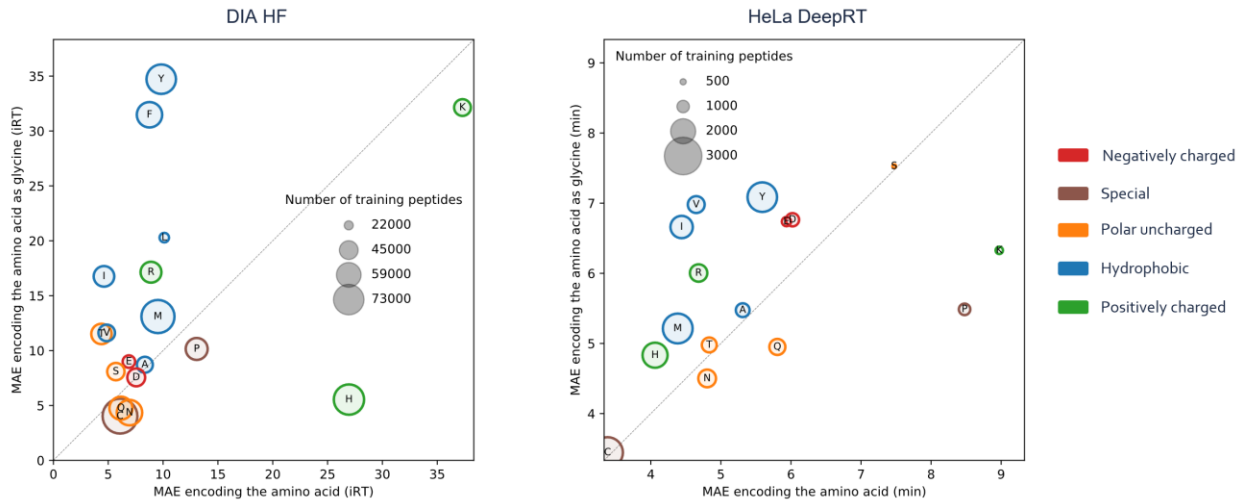

Figure 5: Each amino acid that was excluded for training is shown as a circle, where the size of the circle and color indicates the remaining training peptides and chemical property, respectively. The amino acid is either encoded as glycine (vertical axis) or as its own atomic composition (horizontal axis) and its position depicts the MAE for all amino acid containing peptides. This means that everything above the diagonal line is predicted with a higher accuracy when the amino acid is encoded as itself, while the reverse is true if it is below the diagonal line.

Evaluation of open modification identifications

Predicted retention times have the potential to overcome the identification ambiguity issue[26,27]. Because of DeepLC's unique capability to accurately predict retention times of (unseen) modifications, these predictions can be applied to open modification searches, where identification ambiguity is a key problem[21]. Indeed, open searches introduce considerable ambiguity through the very large number of possible modifications considered, which can be reduced through orthogonal measurements such as retention time.

DeepLC was applied on the results of an open modification search of CD8-positive T-cell data[28] using the pFind[22] search engine. Figure 6A shows observed retention time plotted against predicted retention time for the resulting peptide spectrum matches (PSMs). While the retention time is accurately predicted for PSMs with a Q-value lower than 0.01, much higher retention time

273 errors are observed for PSMs with q-values higher than or equal to 0.01. Figure 6B shows that
274 these PSMs do have a higher error, but the mode is still around zero. This indicates that we mostly
275 expect false identifications to have their mode around zero with a large deviation from this mode.

276 The error distribution of filtered PSMs (Q-value >= 0.01) is now compared to distributions of
277 selected modifications to flag suspect modification groups. Boxplots of the error distributions for
278 four subsets of modifications are shown in Figure 6C. The subset containing the ten most found
279 modifications all show a low error spread that is within 5% of the maximum elution time (300
280 seconds) and is generally centered around zero. The subset of modifications with the largest errors
281 are in the range of 25% of the maximum elution time (1500 seconds) and are mostly centered
282 around zero seconds. A notable exception is dethiomethyl with a shifted median retention time
283 error of 1000 seconds. This shift can be explained by in-source fragmentation, which causes
284 oxidized methionine to lose its side chain[29]. If in-source fragmentation is the cause than the
285 observed retention times are expected to be based on the oxidized methionine equivalent. To
286 verify whether this is the case, PSMs with dethiomethyl were replaced with their oxidized
287 methionine precursors. Figure 6D shows that replacing detiomethyl with oxidized methionine
288 reduces the predicted retention time error to around the same level as expected for oxidized
289 methionine peptides in Figure 6C.

290 The subset of modifications with large errors shows very similar patterns to the next subset, which
291 contains modifications that are not expected to occur in the sample, as these are experimentally
292 induced and thus should not be found in the untreated biological sample under analysis here. In

293 effect, the similarity between these two subsets of modifications indicates that modifications with
294 large retention time errors according to DeepLC can be flagged as highly suspect.

295 Finally, the last subset singles out presumed detection of mutations, which show similar or worse
296 error distributions than the previous two subsets. The large error hints at an incorrect
297 interpretation of the observed mass shift. For these incorrect interpretations one could expect
298 bimodal distributions that contain a combination of right and wrongly assigned mass shifts, but
299 the error distributions are mostly unimodal. The observation that presumed mutations are among
300 the most problematic corresponds to the known non-trivial nature of reliably identifying such
301 sequence changes[26,30].

302 These results thus demonstrate that the unique capabilities of DeepLC allow it to be used as an
303 orthogonal measure to flag suspect identifications in open modification searches.

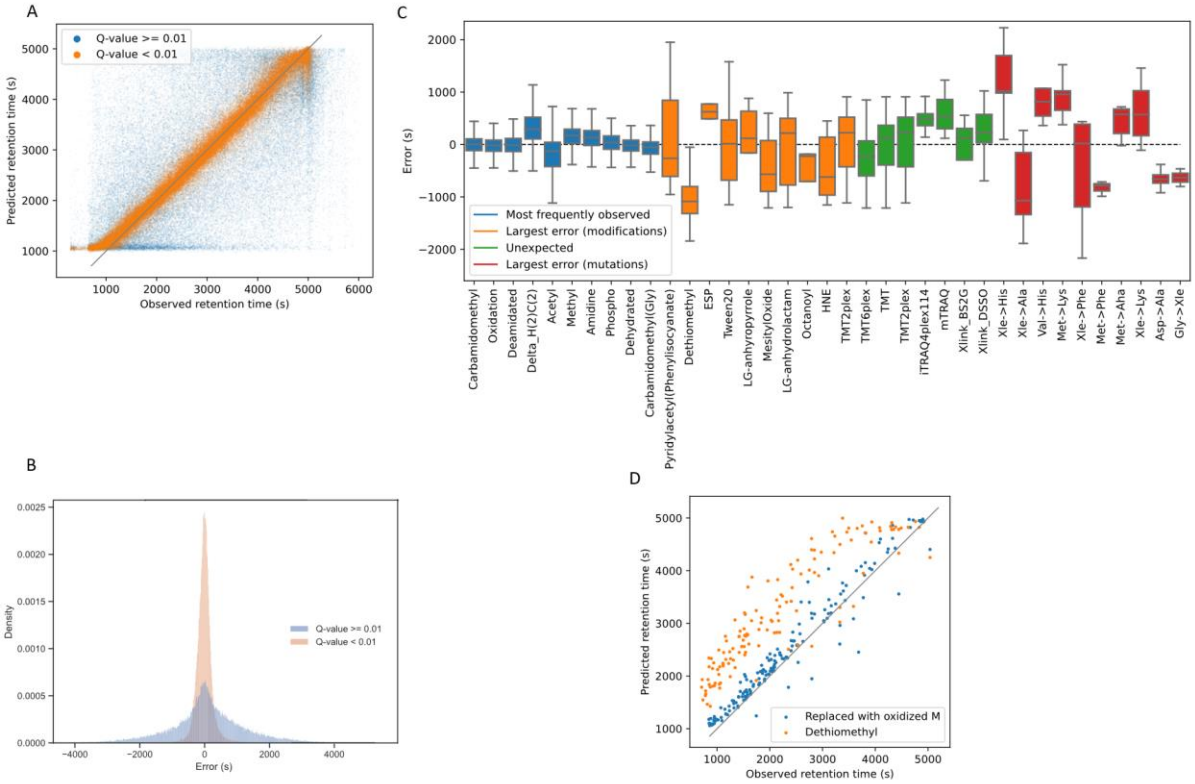

Figure 6: Predicted retention time analysis for open modification results of a CD8-positive T-cell data set. (A) Predicted and observed retention times split by Q-value. Panel (B) shows the error distribution split by Q-value and any points that are higher than 1.5 times the interquartile range plus the relevant quartile range are excluded from the plot. Panel (C) only shows PSMs with Q-values < 0.01. Colors indicate four different subsets of detected modifications. (1) PSMs carrying the top ten most abundant modifications (2) PSMs carrying the ten modifications with the largest absolute mean error (3) PSMs carrying modifications that are not expected to occur in the sample; and (4) PSMs carrying the top ten mutations with the largest absolute mean error. Panel (D) contains PSMs that were identified to contain a dethiomethyl modification and predictions for the same peptides where the dethiomethyl is replaced with an oxidation.

Discussion & Conclusion

Our evaluation shows that DeepLC performs similarly to current state-of-the-art models for unmodified peptides. DeepLC performance furthermore increases for larger data sets, where models trained on larger data sets can provide accurate predictions for smaller data sets. More importantly, DeepLC can accurately predict the retention time of modified peptides, even for modifications that were not included in the training set. This ability to predict for unseen

319 modifications was evaluated with a two-pronged evaluation strategy using both unmodified
320 peptides as well as synthetic, modified peptides. For both evaluations encoding modifications for
321 prediction improves performance, while performance is reduced only for specific modifications
322 that are very different from any other structure in the data set. Finally, the potential of this unique
323 capability of DeepLC is illustrated through its ability to flag suspect PSMs in an open modification
324 search. Crucially, DeepLC showed much larger prediction errors for PSMs that carried
325 modifications that are certain to be absent from the sample.

326 Future development of models that can predict the retention time for unseen modifications could
327 focus on structural aspects of modifications. DeepLC is currently limited in differentiating between
328 isomeric structures that are physicochemically different. Indeed, the observation that structure,
329 not only atomic composition, leads to the physicochemical properties of molecules has already
330 been observed for small molecules. Here, the decision was made to work with atomic composition,
331 because of the ready availability of the composition in databases like Unimod, and greater ease
332 of integration when compared to more complex structural descriptors.

333 DeepLC enables the field to generate predictions for a wide landscape of modification. In order
334 to improve the availability to researchers and their use-cases, DeepLC is made freely available
335 online and has a user-friendly GUI. Furthermore, the tool is available in code repositories that
336 enable easy incorporation in workflows and pipelines for automatic predictions.

Methods

Architecture

DeepLC uses a convolutional deep learning architecture with four different paths for a given encoded peptide. The same peptide acts as the input for the four paths, which have multiple separated layers, as shown in Figure 7. Three of the initial paths use a combination of convolutional[31] and max pooling layers[32]. The remaining path, which propagates global features, consists of densely connected layers. The results of all initial four paths are flattened and concatenated to provide an input for the final combined path which consists of six connected dense layers. A detailed visualization of the architecture is available in Supplementary Figure 7.

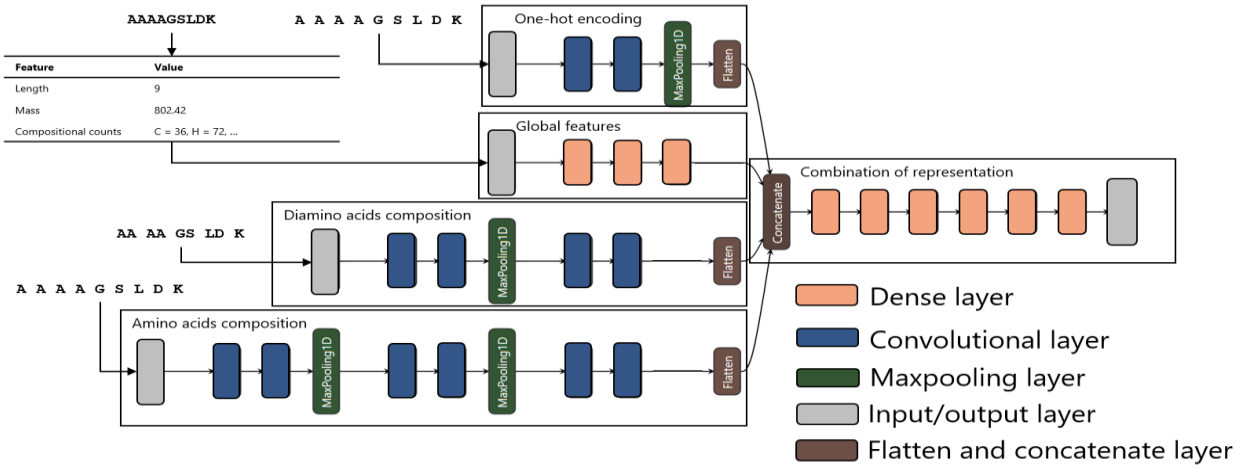

Figure 7: Visualization of DeepLC's convolutional architecture with the four individual paths named: *One-hot encoding*, *Global features*, *Diamino acids composition*, and *Amino acids composition*. These individual paths are concatenated in the *Combination of representations* path.

The input matrix for the *Amino acids composition* path has a dimension of 60 for the peptide sequence by 7 for the atom counts (C, H, N, O, P, and S). Not every peptide is 60 amino acids long, thus "X"-characters without atomic composition are padded to reach 60 amino acids. This implies

353 that encoding modified amino acids becomes straightforward, as computing their atomic
354 composition is trivial. Note that for modified amino acids the atomic composition of the
355 modification is added to the atomic composition of the unmodified residue. This encoding allows
356 the model to learn patterns that generalize to unseen modifications.

357 The *Diamino acid* path was added to further improve the generalization capability of the model.
358 In this layer the peptide is divided into diamino acids without overlap. This improves the
359 generalization capability, as the input values for each position are more thoroughly represented.
360 Otherwise there would only be 20 unmodified amino acid representations, combined with a
361 limited amount of modifications. Besides interpreting the amino acids in pairs, the *Diamino acid*
362 path uses the same logic as the *Amino acids composition* path, leading to an input matrix of 30
363 paired positions by 6 atoms.

364 Encoding amino acids and their modifications by strictly using the atomic composition does,
365 however, not allow for comprehensively capturing all molecular information. Indeed, the structure
366 of isomers can play an important role in the physicochemical properties of amino acids, as is
367 exemplified by structural isomers isoleucine and leucine[33]. This is the reason that one-hot
368 encoding of unmodified amino acids was still used in DeepLC as an input for the *One-hot encoding*
369 path. However, to reduce the impact of this layer, the number of filters for this path were limited
370 to a mere 2. The dimensions of this input matrix is 60 positions by 20 amino acids.

371 In addition to all paths that encode position specific information, the *Global features* path takes
372 global information of the peptide into account. These global features include the length and total
373 atomic composition of the peptide. The dimension of this input vector is 7.

374 Three versions of the model were trained, solely differing in kernel size (of 2, 4, and 8) for the
375 *Amino acids composition* path. These three models were combined in an ensemble by averaging
376 their predictions.

377 Finally, the other hyperparameters of each layer in DeepLC are consistent for all versions with
378 different kernel sizes. All layers, except the output layer and the *One-hot encoding* path, use L1
379 regularization with $\alpha = 2.5e - 7$ and a leaky ReLU[34] with a maximum activation value of 20. The
380 *One-hot encoding* path uses the tanh activation function, as within this path we are only interested
381 in the ability to separate unmodified amino acid isomers.

382 Data sets & evaluation

383 To evaluate the generalization performance of DeepLC, we selected 20 data sets from a wide
384 variety of organisms and experimental setups (Supplementary Table 2). We further selected three
385 data sets (*SWATH Library*[35], *HeLa HF*[36], and *DIA HF*[37]) for detailed result reporting, with the results
386 for the other 17 data sets described in the supplementary information. The data sets *SWATH*
387 *Library* and *DIA HF* were selected based on their previous use by Ma *et al.* for DeepRT[11] and by
388 Guan *et al.*[9], respectively. A third data set, *HeLa HF* was selected because of its use of short
389 (compared to other used data sets) gradients of 15 minutes and the large number of training
390 peptides.

391 The variety in experimental setups and protocols means that the acquired and predicted retention
392 times need to be calibrated. The *ProteomeTools library*[38], *SWATH Library*, and *DIA HF* data sets
393 were normalized to the iRT peptides[39,40]. DeepLC itself supports linear calibration which is further
394 explained in the online DeepLC documentation.

395 The data sets marked *Custom workflow* in Supplementary Table 2 were processed as follows. Raw
396 mass spectrometry files were downloaded from PRIDE Archive[41] and converted to MGF format
397 with the ThermoRawFileParser[42]. These were then searched using the MS-GF+ search engine[43]
398 with a concatenated target-decoy sequence database containing the respective species'
399 UniProtKB proteome and the common Repository of Adventitious Proteins (cRAP:
400 https://www.thegpm.org/crap/). The MS-GF+ search results were post-processed with
401 Percolator[44] to a false discovery rate of 0.01. Retention times were parsed from the MGF files for
402 all confidently identified peptides. Within each LC-MS run, the median retention time for each
403 peptidoform (peptide - modifications combination) was calculated. All median retention times
404 were then linearly calibrated across all LC-MS runs for each data set, using the shared
405 peptidoforms as anchor points. Finally, the median calibrated retention time was calculated for
406 each peptidoform across all runs for each data set. These median calibrated retention times were
407 then used to train, validate and test DeepLC. The steps comprising this calibration are available in
408 a Snakemake workflow[45].

409 The data sets marked *Custom workflow ProteomeTools* in Supplementary Table 2 were processed
410 as follows. MaxQuant[46] identification files were filtered on posterior error probabilities < 0.01 and
411 scores > 90. The retention times were calibrated with the peptides in Supplementary Table 3.
412 Within a run, the median retention time per peptidoform was used for further analysis. Then,
413 across runs the median retention time per peptidoform was taken for the final retention time.

414 The data sets marked *Custom workflow ProteomeTools PTM*[25] in Supplementary Table 2 were
415 processed in the same way as the data sets *Custom workflow ProteomeTools*, with the only
416 exception that the retention times were calibrated with the peptides in Supplementary Table 4.

417 Each data set was split into a test set (10%), validation set (5%), and training set (85%). The
418 validation set is used for model selection only, while all performance results presented here were
419 computed from the test set. Prediction performance is measured using three commonly used
420 metrics: Mean Absolute Error (MAE), Pearson correlation, and $\Delta t_{95\%}$. The latter describes the error
421 for a retention time window that contains 95% of the peptides in the error distribution. To make
422 the MAE and $\Delta t_{95\%}$ comparable between experiments, we divided them by the retention time of
423 the last detected peptide in the respective data set. These metrics are further referred to as relative
424 MAE and relative $\Delta t_{95\%}$.

425 Open modification search

426 Results from an open modification search by pFind[26] are used to evaluate the ability of DeepLC to
427 identify suspect identifications. Open modification searches are particularly prone to falsely
428 identify modified peptides due to the larger search space and resulting identification ambiguity[46].
429 The search was performed on a data set on CD8-positive T cells by Kim *et al.*[28], obtained from the
430 PRIDE repository[47] with identifier PXD000561. The search was run with pFind version 3.1.5. Search
431 parameters were set to: 20ppm precursor mass error tolerance, peptide length limit from 7 to 30
432 amino acids, modifications were limited to mass deltas from -150 to 500 Dalton, a maximum of
433 two miss-cleavages were allowed, and oxidation of M and carbamidomethylation of C were set as
434 variable modifications.

Software and scripts

The following Python libraries were used in DeepLC: Pandas[48], TensorFlow[49], Pyteomics[50], SciPy[51], and Numpy[52]. The code used to prepare the data sets, calibrate retention times, generate DeepLC models, make predictions, and generate the figures is available on Zenodo: https://zenodo.org/record/4542884.

For the DeepLC tool (Supplementary Figure 8) itself, see Availability.

Availability

DeepLC is available for download from the following repositories and package indexes:

- Graphical user interface: https://github.com/compomics/DeepLC/releases/latest
- Python package: https://pypi.org/project/deeplc/
- Bioconda package: https://bioconda.github.io/recipes/deeplc/README.html
- Biocontainers docker image: https://quay.io/repository/biocontainers/deeplc
- Source code: https://github.com/compomics/DeepLC

Acknowledgements

R.B. acknowledges funding from the Marie Sklodowska-Curie EU Framework for Research and Innovation Horizon 2020 MASSTRPLAN [675132] and Vlaams Agentschap Innoveren en Ondernemen under project number HBC.2020.2205; R.G. acknowledges funding from the Research Foundation Flanders (FWO) [1S50918N]; S.D. and L.M. acknowledge funding from the European Union's Horizon 2020 Programme (H2020-INFRAIA-2018-1) [823839]; N.H. and L.M. acknowledge funding from the Research Foundation Flanders (FWO) [G042518N].

Competing interests

The authors declare no competing interests.

Contributions

R.B., R.G., and S.D. conceived the study. R.B., R.G., L.M. and S.D. designed the experiments, analyzed the results, and wrote the manuscript. R.G. made the tool available in python package repositories. N.H. and R.B. build the graphical user interface.

References

1. Aebersold, R. & Mann, M. Mass spectrometry-based proteomics. *Nature* vol. 422 198–207 (2003).
2. Shishkova, E., Hebert, A. S. & Coon, J. J. Now, More Than Ever, Proteomics Needs Better Chromatography. *Cell Systems* vol. 3 321–324 (2016).
3. Michalski, A., Cox, J. & Mann, M. More than 100,000 detectable peptide species elute in single shotgun proteomics runs but the majority is inaccessible to data-dependent LC-MS/MS. *J. Proteome Res.* **10**, 1785–1793 (2011).
4. Moruz, L. & Käll, L. Peptide retention time prediction. *Mass Spectrom. Rev.* **36**, 615–623 (2017).
5. Reimer, J., Spicer, V. & Krokhin, O. V. Application of modern reversed-phase peptide retention prediction algorithms to the Houghten and DeGraw dataset: Peptide helicity and its effect on prediction accuracy. *J. Chromatogr. A* **1256**, 160–168 (2012).
6. Searle, B. C. *et al.* Chromatogram libraries improve peptide detection and quantification by data independent acquisition mass spectrometry. *Nat. Commun.* **9**, 1–12 (2018).
7. Guo, D., Mant, C. T., Taneja, A. K. & Hodges, R. S. Prediction of peptide retention times in reversed-phase high-performance liquid chromatography II. Correlation of observed and predicted peptide retention times factors and influencing the retention times of peptides. *J. Chromatogr. A* **359**, 519–532 (1986).
8. Moruz, L. *et al.* Chromatographic retention time prediction for posttranslationally modified peptides. *Proteomics* **12**, 1151–1159 (2012).
9. Guan, S., Moran, M. F. & Ma, B. Prediction of LC-MS/MS properties of peptides from sequence by deep learning. *Mol. Cell. Proteomics* **18**, 2099–2107 (2019).
10. Gessulat, S. *et al.* Prosit: proteome-wide prediction of peptide tandem mass spectra by deep learning. *Nat. Methods* **16**, 509–518 (2019).
11. Ma, C. *et al.* Improved Peptide Retention Time Prediction in Liquid Chromatography

487 through Deep Learning. *Anal. Chem.* **90**, 10881–10888 (2018).

488 12. Palmblad, M., Ramström, M., Markides, K. E., Håkansson, P. & Bergquist, J. Prediction of
489 Chromatographic Retention and Protein Identification in Liquid Chromatography/Mass
490 Spectrometry. *Anal. Chem.* **74**, 5826–5830 (2002).

491 13. MacLean, B. *et al.* Skyline: an open source document editor for creating and analyzing
492 targeted proteomics experiments. *Oxford* **26**, 1401–1403 (2017).

493 14. C Silva, A. S. *et al.* Accurate peptide fragmentation predictions allow data driven approaches
494 to replace and improve upon proteomics search engine scoring functions. *Bioinformatics*
495 **35**, 1401–1403 (2019).

496 15. Bertsch, A. *et al.* Optimal de novo design of MRM experiments for rapid assay development
497 in targeted proteomics. *J. Proteome Res.* **9**, 2696–704 (2010).

498 16. Dorfer, V., Maltsev, S., Winkler, S. & Mechtler, K. CharmeRT: Boosting Peptide Identifications
499 by Chimeric Spectra Identification and Retention Time Prediction. *J. Proteome Res.* **17**,
500 2581–2589 (2018).

501 17. Van Puyvelde, B. *et al.* Removing the Hidden Data Dependency of DIA With Predicted
502 Spectral Libraries. *Proteomics* **20**, 1900306 (2020).

503 18. Yang, Y. *et al.* In silico spectral libraries by deep learning facilitate data-independent
504 acquisition proteomics. *Nat. Commun.* **11**, 1–11 (2020).

505 19. Searle, B. C. *et al.* Generating high quality libraries for DIA MS with empirically corrected
506 peptide predictions. *Nat. Commun.* **11**, 1548 (2020).

507 20. Bittremieux, W., Meysman, P., Noble, W. S. & Laukens, K. Fast Open Modification Spectral
508 Library Searching through Approximate Nearest Neighbor Indexing. *J. Proteome Res.* **17**,
509 3463–3474 (2018).

510 21. Kong, A. T., Leprevost, F. V, Avtonomov, D. M., Mellacheruvu, D. & Nesvizhskii, A. I.
511 MSFragger: ultrafast and comprehensive peptide identification in mass spectrometry–
512 based proteomics. *Nat. Methods* **14**, 513–520 (2017).

513 22. Chi, H. *et al.* Comprehensive identification of peptides in tandem mass spectra using an
514 efficient open search engine. *Nat. Biotechnol.* **36**, 1059–1066 (2018).

515 23. Na, S., Bandeira, N. & Paek, E. Fast multi-blind modification search through tandem mass
516 spectrometry. **11**, M111.010199 (2012).

517 24. Creasy, D. M. & Cottrell, J. S. Unimod: Protein modifications for mass spectrometry.
518 *Proteomics* **4**, 1534–1536 (2004).

519 25. Paul Zolg, D. *et al.* Proteometools: Systematic characterization of 21 post-translational
520 protein modifications by liquid chromatography tandem mass spectrometry (lc-ms/ms)
521 using synthetic peptides. *Mol. Cell. Proteomics* **17**, 1850–1863 (2018).

522 26. Colaert, N., Degroeve, S., Helsens, K. & Martens, L. Analysis of the resolution limitations of
523 peptide identification algorithms. *J. Proteome Res.* **10**, 5555–5561 (2011).

524 27. Bouwmeester, R., Gabriels, R., Van Den Bossche, T., Martens, L. & Degroeve, S. The Age of
525 Data-Driven Proteomics: How Machine Learning Enables Novel Workflows. *Proteomics* **20**,
526 1900351 (2020).

527 28. Kim, M. S. *et al.* A draft map of the human proteome. *Nature* **509**, 575–581 (2014).

528 29. Müller, T. & Winter, D. Systematic evaluation of protein reduction and alkylation reveals
529 massive unspecific side effects by iodine-containing reagents. *Mol. Cell. Proteomics* **16**,
530 1173–1187 (2017).

531 30. Salz, R. *et al.* The Personalized Proteome: Comparing Proteogenomics and Open Variant
532 Search Approaches for Single Amino Acid Variant Detection. *bioRxiv* 2020.12.11.419523
533 (2020) doi:10.1101/2020.12.11.419523.

534 31. Fukushima, K. Neocognitron: A hierarchical neural network capable of visual pattern
535 recognition. *Neural Networks* **1**, 119–130 (1988).

536 32. Ranzato, M., Huang, F., … Y. B.-2007 I. conference & 2007, undefined. Unsupervised
537 learning of invariant feature hierarchies with applications to object recognition.
538 *ieeexplore.ieee.org*.

539 33. Parker, J. M. R., Guo, D. & Hodges, R. S. New Hydrophilicity Scale Derived from High-
540 Performance Liquid Chromatography Peptide Retention Data: Correlation of Predicted
541 Surface Residues with Antigenicity and X-ray-Derived Accessible Sites. *Biochemistry* **25**,
542 5425–5432 (1986).

543 34. Nair, V. & Hinton, G. E. *Rectified Linear Units Improve Restricted Boltzmann Machines*.
544 *cs.toronto.edu* https://www.cs.toronto.edu/~hinton/absps/reluICML.pdf.

545 35. Rosenberger, G. *et al.* A repository of assays to quantify 10,000 human proteins by SWATH-
546 MS. *Sci. Data* **1**, (2014).

547 36. Kelstrup, C. D. *et al.* Performance Evaluation of the Q Exactive HF-X for Shotgun Proteomics.
548 *J. Proteome Res.* **17**, 727–738 (2018).

549 37. Bruderer, R. *et al.* Optimization of Experimental Parameters in Data-Independent Mass
550 Spectrometry Significantly Increases Depth and Reproducibility of Results. *Mol. Cell.*
551 *Proteomics* **16**, 2296–2309 (2017).

552 38. Zolg, D. P. *et al.* Building ProteomeTools based on a complete synthetic human proteome.
553 *Nat. Methods* **14**, 259–262 (2017).

554 39. Escher, C. *et al.* Using iRT, a normalized retention time for more targeted measurement of
555 peptides. *Proteomics* **12**, 1111–1121 (2012).

556 40. Zolg, D. P. *et al.* PROCAL: A Set of 40 Peptide Standards for Retention Time Indexing,

Column Performance Monitoring, and Collision Energy Calibration. *Proteomics* **17**, 1700263 (2017).

41. Martens, L. *et al.* PRIDE: The proteomics identifications database. *Proteomics* **5**, 3537–3545 (2005).

42. Hulstaert, N. *et al.* ThermoRawFileParser: Modular, Scalable, and Cross-Platform RAW File Conversion. *J. Proteome Res.* **19**, 537–542 (2020).

43. Kim, S. & Pevzner, P. A. MS-GF+ makes progress towards a universal database search tool for proteomics. *Nat. Commun.* **5**, 5277 (2014).

44. Käll, L., Canterbury, J. D., Weston, J., Noble, W. S. & MacCoss, M. J. Semi-supervised learning for peptide identification from shotgun proteomics datasets. *Nat. Methods* **4**, 923–925 (2007).

45. Köster, J. & Rahmann, S. Snakemake—a scalable bioinformatics workflow engine. *Bioinformatics* **28**, 2520–2522 (2012).

46. Cox, J. & Mann, M. MaxQuant enables high peptide identification rates, individualized p.p.b.-range mass accuracies and proteome-wide protein quantification. *Nat. Biotechnol.* **26**, 1367–1372 (2008).

47. Vizcaíno, J. A. *et al.* ProteomeXchange provides globally coordinated proteomics data submission and dissemination. *Nat. Biotechnol.* **32**, 223–226 (2014).

48. McKinney, W. pandas: a Foundational Python Library for Data Analysis and Statistics. *Python High Perform. Sci. Comput.* 1–9 (2011).

49. Abadi, M. *et al. TensorFlow: Large-Scale Machine Learning on Heterogeneous Distributed Systems*. *arxiv.org* www.tensorflow.org.

50. Levitsky, L. I., Klein, J. A., Ivanov, M. V. & Gorshkov, M. V. Pyteomics 4.0: Five Years of Development of a Python Proteomics Framework. *J. Proteome Res.* **18**, 709–714 (2019).

51. Virtanen, P. *et al.* SciPy 1.0: fundamental algorithms for scientific computing in Python. *Nat. Methods* **17**, 261–272 (2020).

52. Oliphant, T. E. *A guide to NumPy*. vol. 1 (Trelgol Publishing USA, 2006).

Supplemental information for:

DeepLC can predict retention times for peptides that carry as-yet unseen modifications

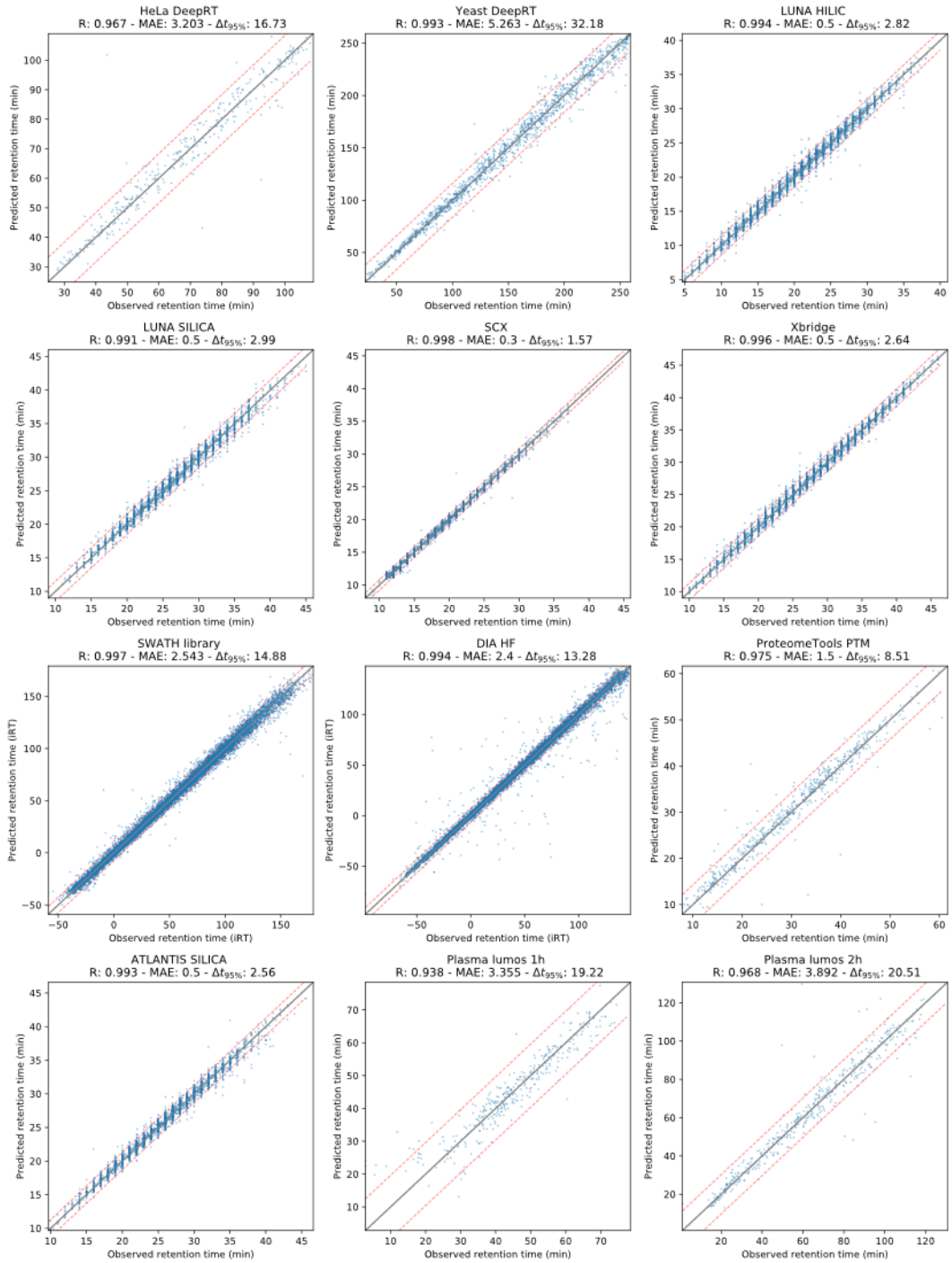

Supplemental Figure 1: Scatter plots for twelve data sets on the test data for each respective data set.

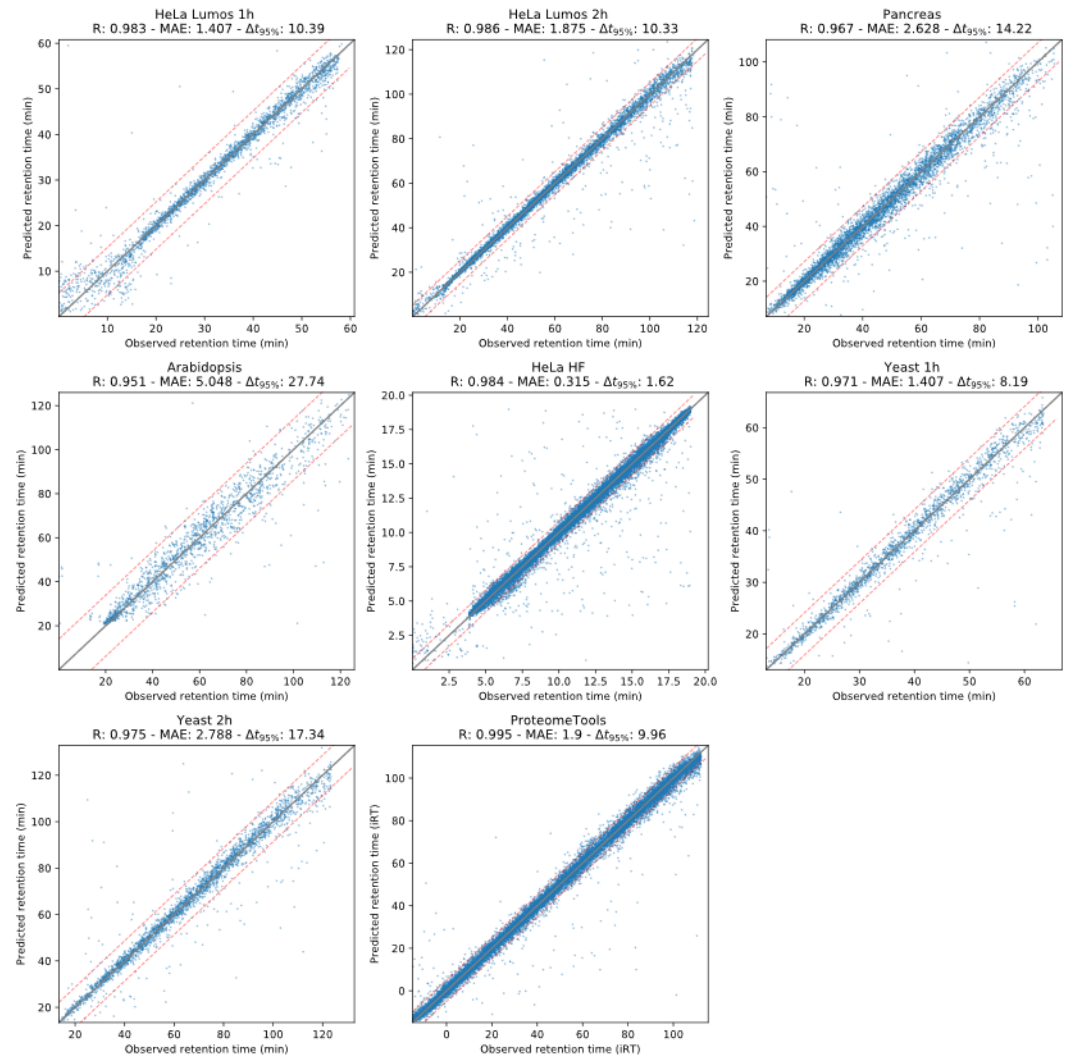

Supplemental Figure 2: Scatter plots for eight data sets on the test data for each respective data set.

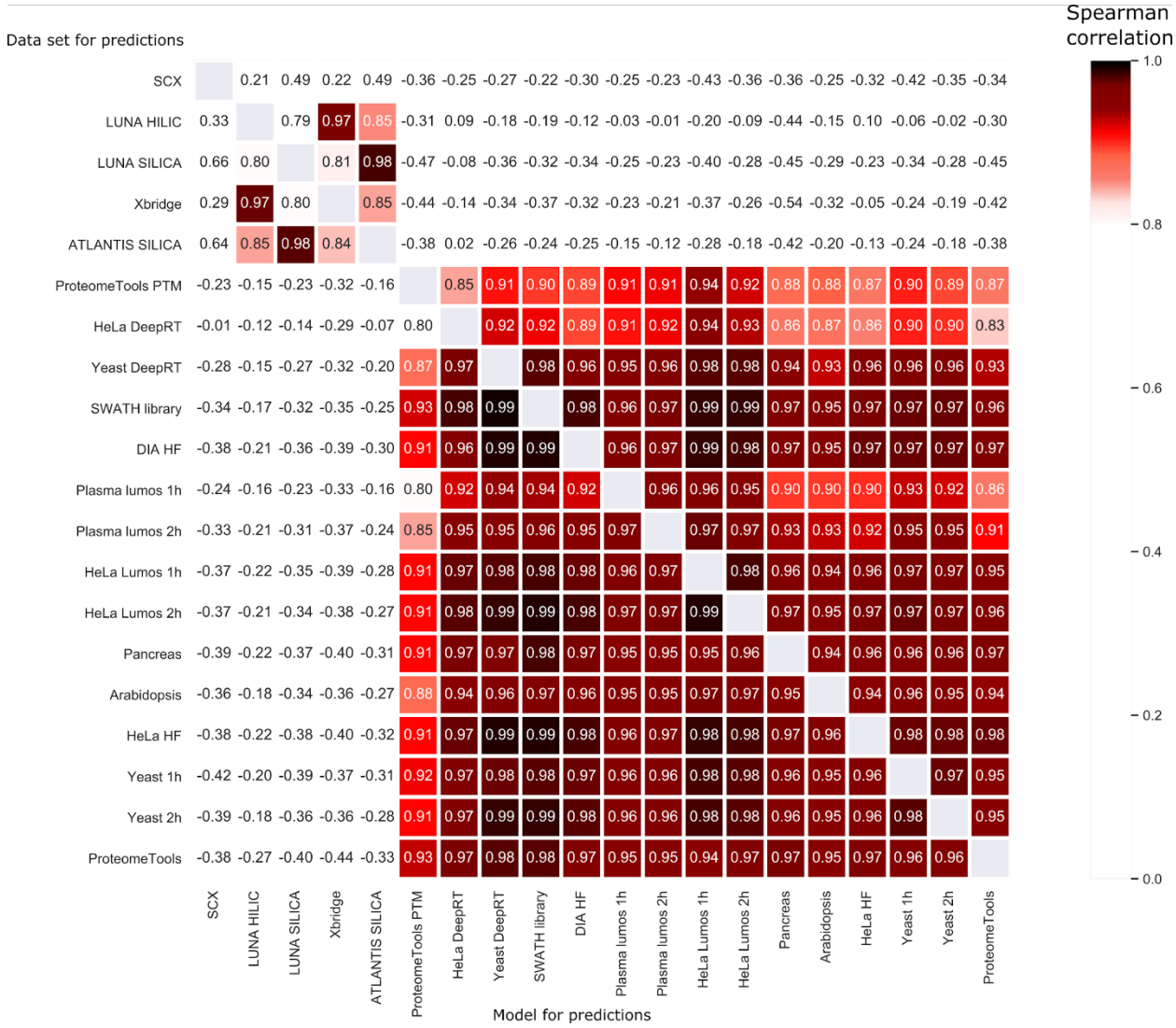

Supplemental Figure 3: Performance in terms of the Spearman correlation for each model applied to the other 19 data sets.

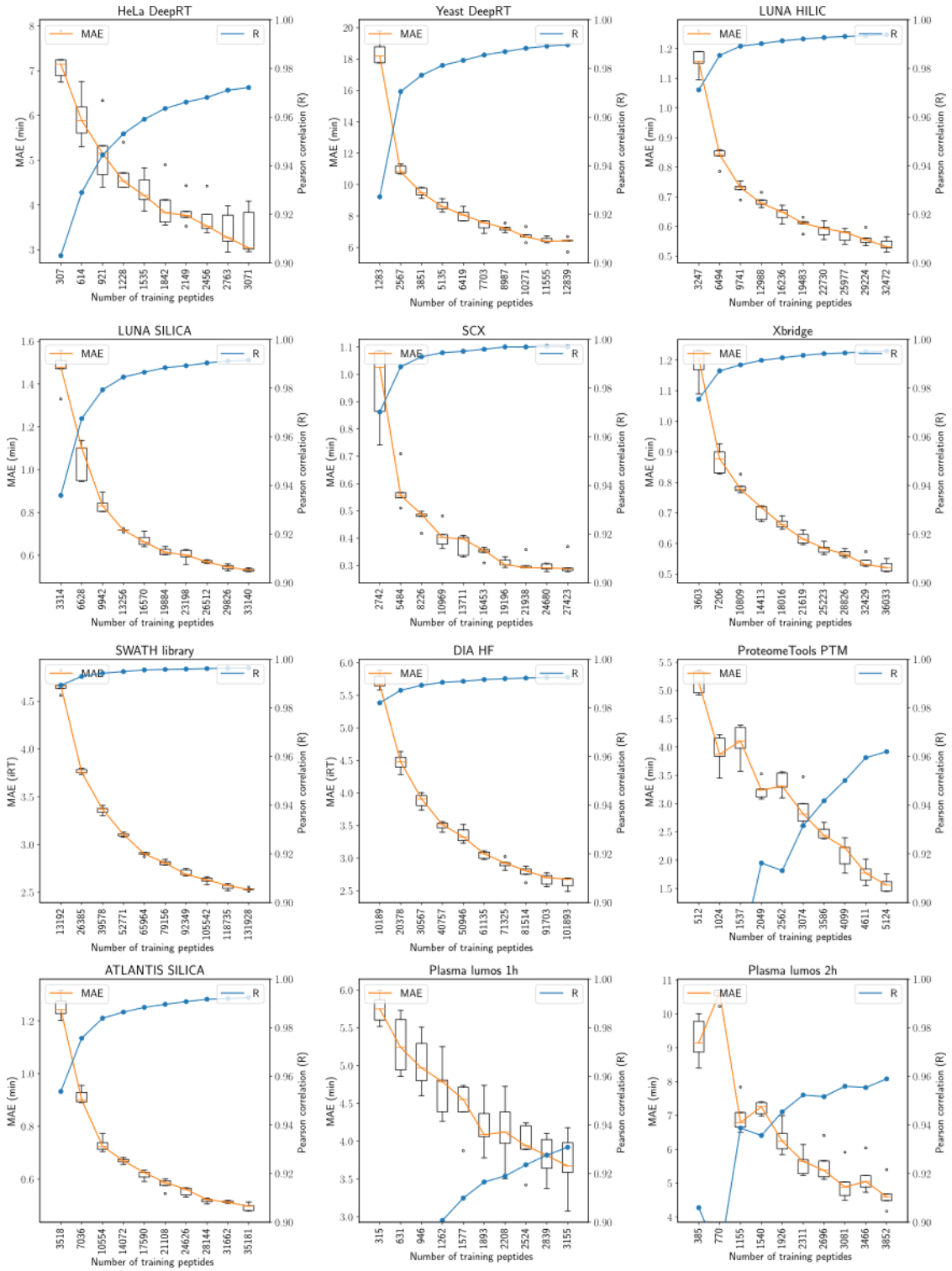

Supplemental Figure 4: Learning curves for twelve data sets with the MAE and correlation between observed and predicted retention times.

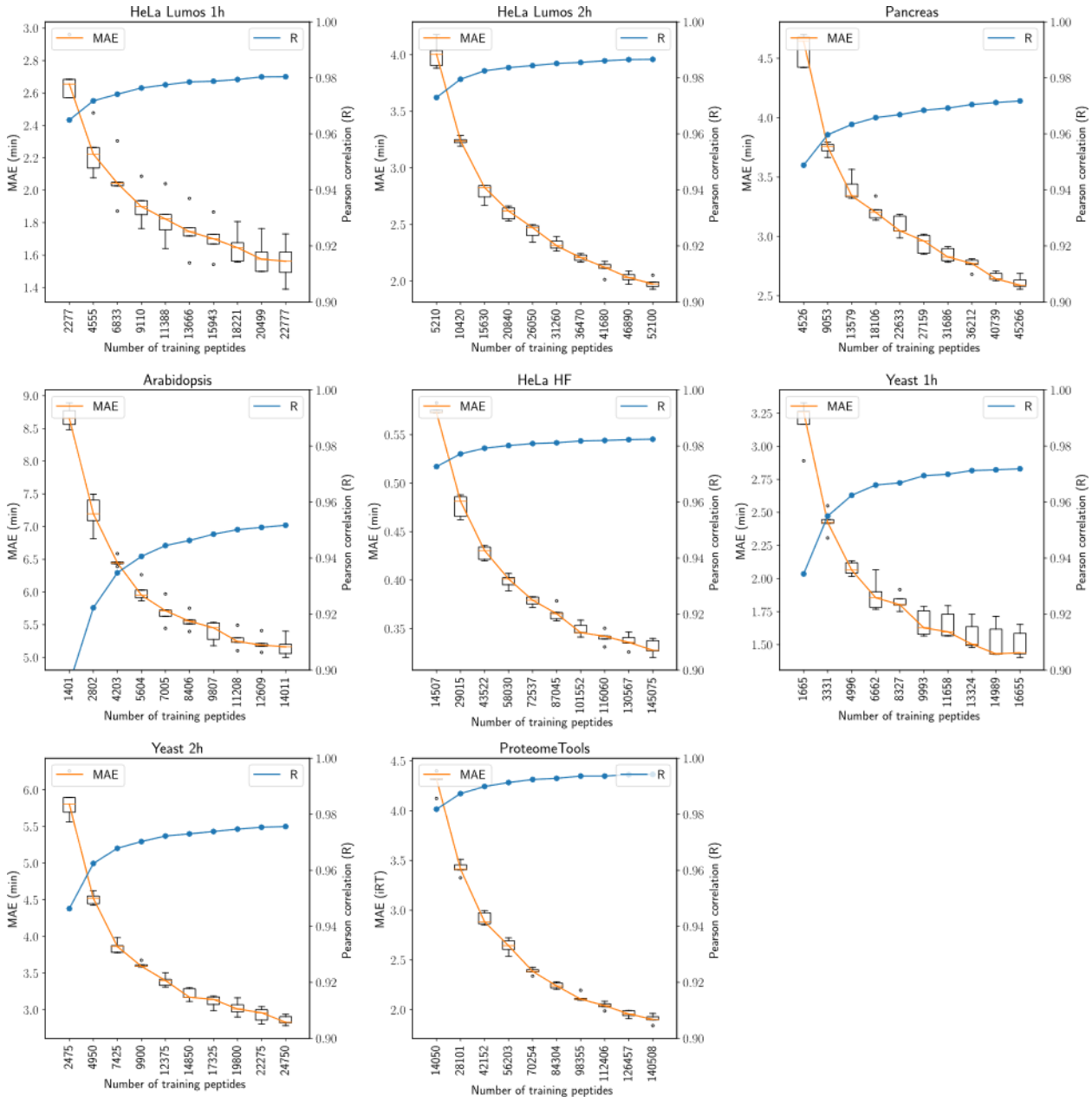

Supplemental Figure 5: Learning curves for eight data sets with the MAE and correlation between observed and predicted retention times.

Supplemental Table 1: Overview of the 20 MS^2 data sets used in this research. The first three columns report test performance for DeepLC. The performance for existing models is listed if available and as reported in the original manuscript (except for the Prosit model where the $\Delta t_{95\%}$ was recalculated based on a digitized version of Figure 1c in the original manuscript). For Guan et al. the $\Delta t_{95\%}$ was recalculated by taking the $\Delta t_{95\%}$ of the absolute error and multiplying this value by two. This value was corrected to be consistent with DeepRT and DeepLC.

Name	**Train peptides**	**Validation peptides**	**Test peptides**	**R**	**MAE**	$\Delta t_{95\%}$	**DeepRT R**	**DeepRT** $\Delta t_{95\%}$	**Guan et al. R**	**Guan et al.** $\Delta t_{95\%}$	**Prosit R**	**Prosit** $\Delta t_{95\%}$
SCX	21638	1138	2530	0.998	0.29	1.57	0.998	1.42				
SWATH library	96798	5094	11321	0.997	2.54	14.88	0.997	13.4				
Xbridge	31483	1656	3682	0.996	0.49	2.64	0.996	2.36				
ProteomeTools	125331	6596	14658	0.995	1.9	9.96					1	8.5
DIA HF	43002	2263	5029	0.994	2.37	13.28			0.994	10.825		
LUNA HILIC	23512	1237	2750	0.994	0.54	2.82	0.994	2.55				
ATLANTIS SILICA	30848	1623	3607	0.993	0.48	2.56	0.995	2.1				
Yeast DeepRT	4867	256	569	0.993	5.26	32.18	0.993	25.88				
LUNA SILICA	26051	1371	3047	0.991	0.54	2.99	0.994	2.3				
HeLa Lumos 2h	34231	1801	4003	0.986	1.87	10.33						
HeLa HF	137821	7253	16119	0.984	0.31	97.04						
HeLa Lumos 1h	13310	700	1556	0.983	1.41	10.39						
ProteomeTools PTM	3659	192	428	0.975	1.54	8.51						
Yeast 2h	15822	832	1850	0.975	2.79	17.34						
Yeast 1h	12197	641	1426	0.971	1.41	8.19						
Plasma lumos 2h	2997	157	350	0.968	3.89	20.51						
HeLa DeepRT	2917	153	341	0.967	3.2	16.73	0.985	12.56				
Pancreas	33421	1759	3909	0.967	2.63	14.22						
Arabidopsis	10132	533	1185	0.951	5.05	27.74						
Plasma lumos 1h	49495	2604	5788	0.938	3.36	19.22						

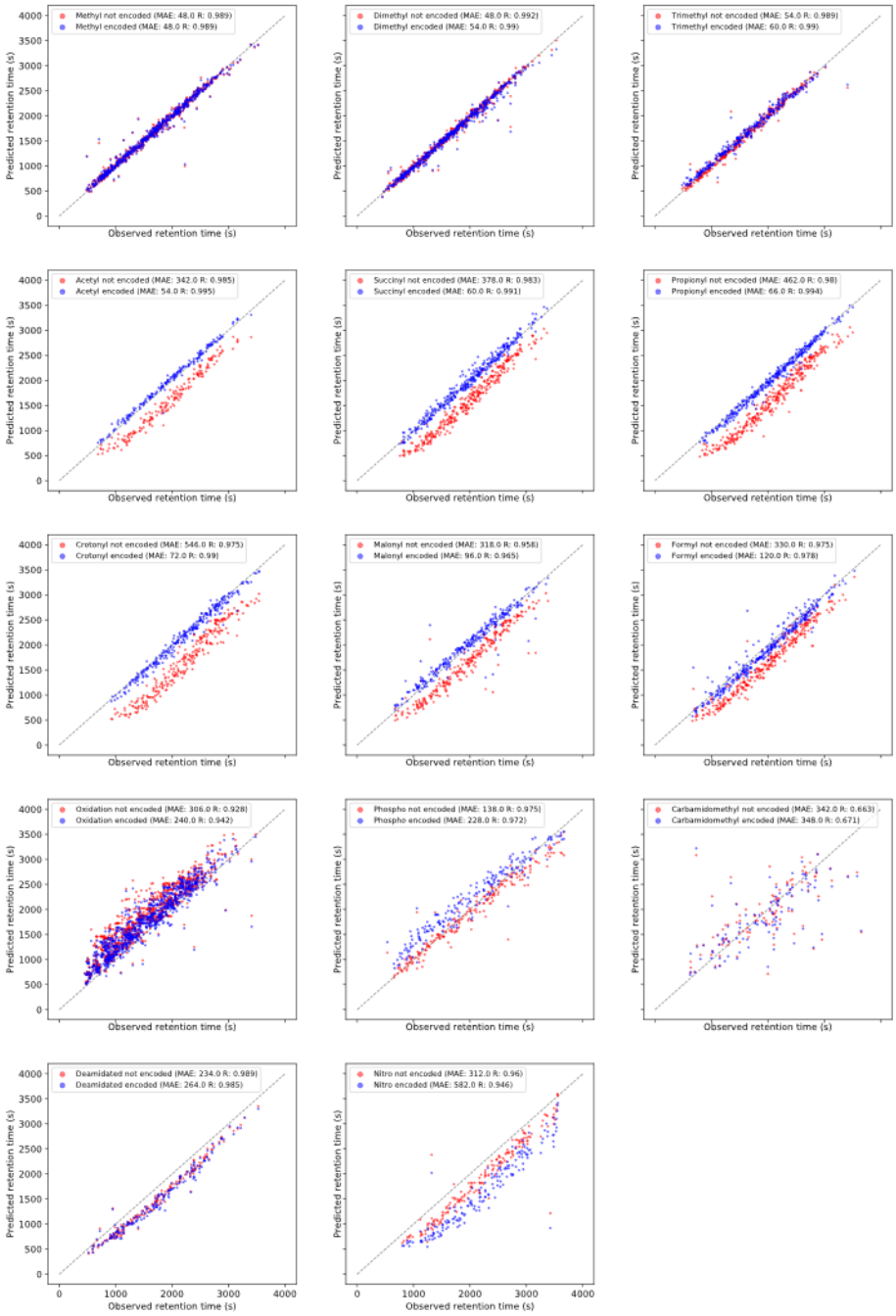

Supplemental Figure 6: Each panel shows the observed retention time against predicted retention time for models that were not trained for the specified modification. Dots show the retention times when modifications are either not encoded (red) or encoded (blue) by DeepLC.

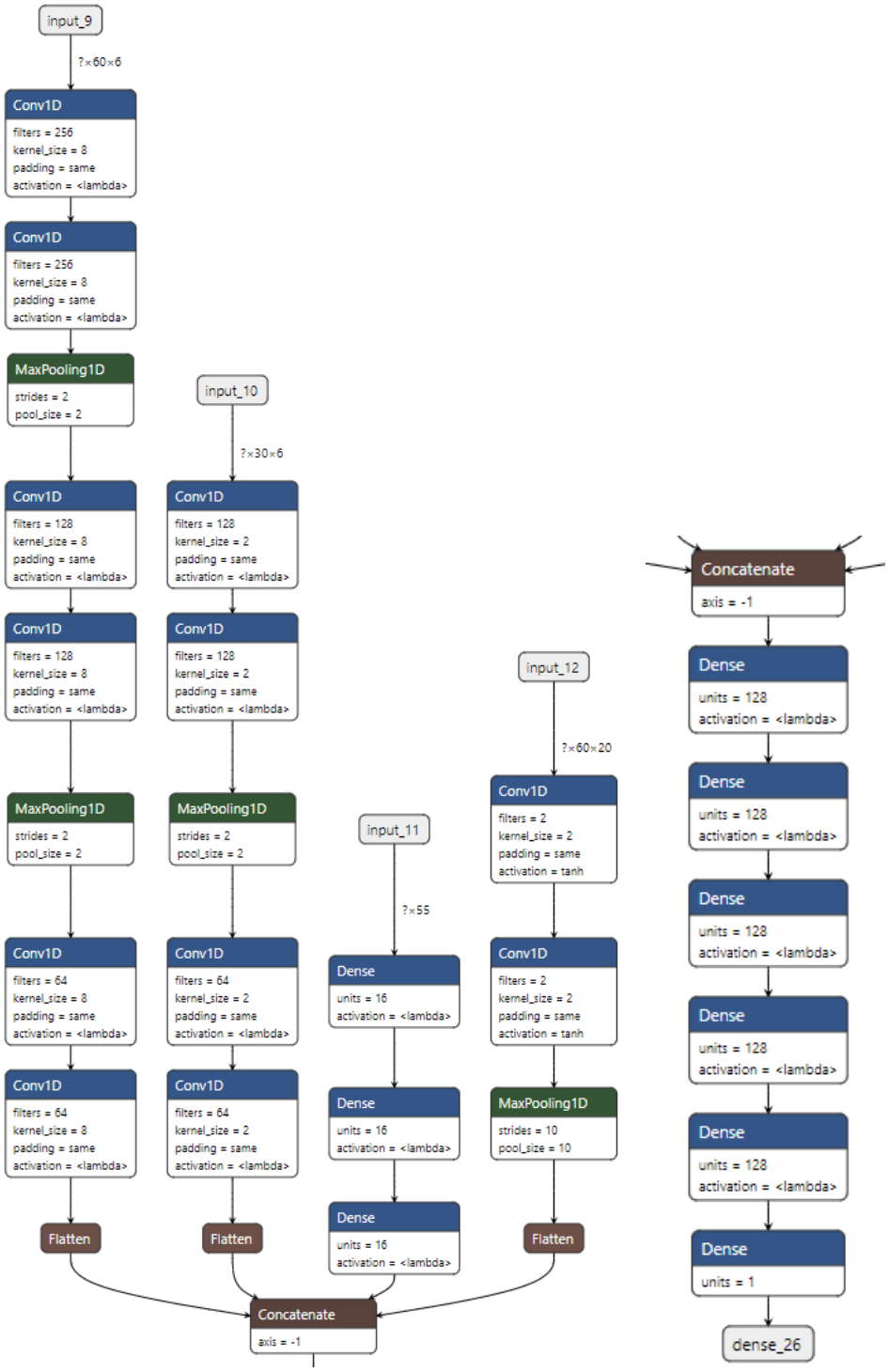

Supplemental Figure 7: Detailed view of the architecture of DeepLC.

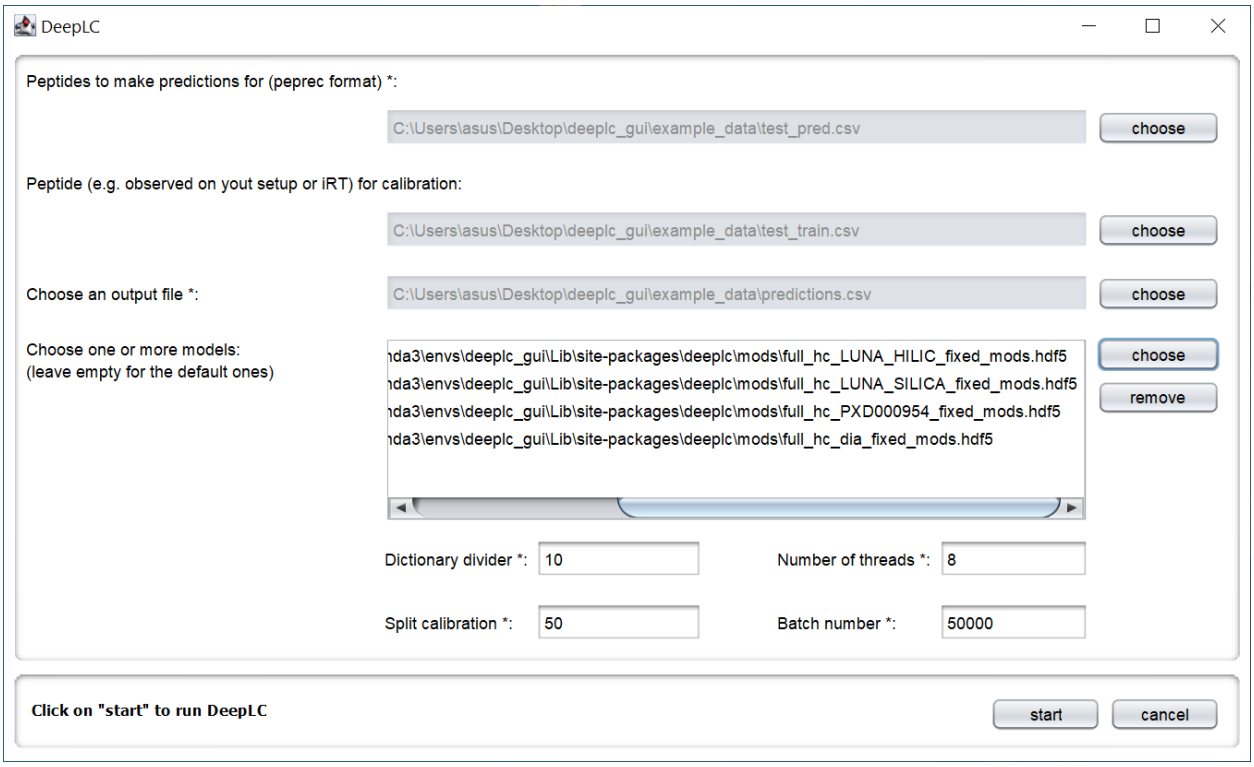

Supplemental Figure 8: Java-based graphical user interface of DeepLC, which allows an easy to use interface to make predictions, with the option to calibrate for the user's experimental setup.

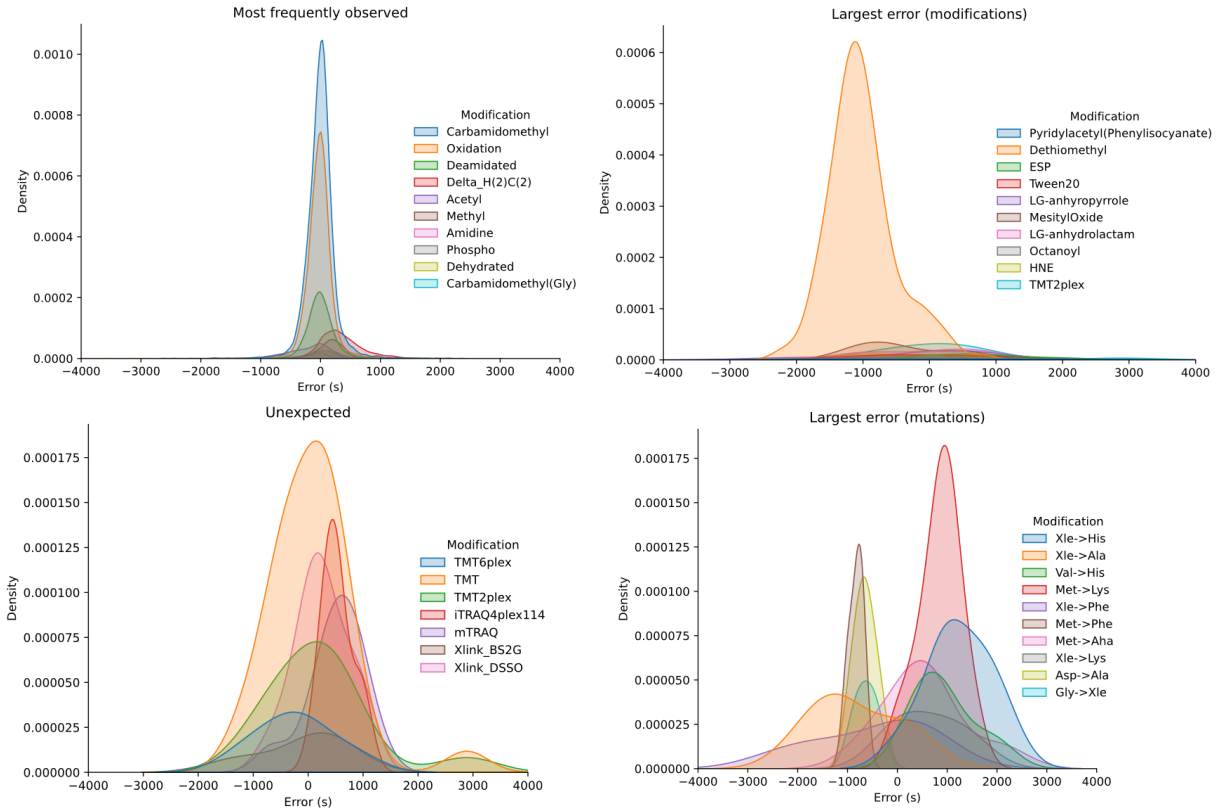

Supplemental Figure 9: Error distribution for four different sets of modifications. (1) PSMs carrying the top ten most abundant modifications (2) PSMs carrying the ten modifications with the largest absolute mean error (3) PSMs carrying modifications that are not expected to occur in the sample; and (4) PSMs carrying the top ten mutations with the largest absolute mean error.

636 Supplemental Table 2: Data sets used to train and evaluate DeepLC

Name	Data origin for fitting	Training peptides	Validation peptides	Test peptides	Repository identifier	Column type
HeLa hf[30]	Custom workflow	137821	7253	16119	PXD006932	RP
ProteomeTools[32]	Custom workflow ProteomeTools	125331	6596	14658	PXD010595; PXD004732	RP
SWATH library[29]	DeepRT[11]	96798	5094	11321	PXD000954	RP
Plasma lumos 1h[47]	Custom workflow	49495	2604	5788	PXD013477	RP
DIA HF[31]	Guan et al.[9]	43002	2263	5029	PXD005573	RP
HeLa lumos 2h[47]	Custom workflow	34231	1801	4003	PXD013477	RP
Pancreas[48]	Custom workflow	33421	1759	3909	PXD010154	RP
Xbridge[49]	DeepRT[11]	31483	1656	3682		HILIC
ATLANTIS SILICA[49]	DeepRT[11]	30848	1623	3607		HILIC
LUNA SILICA[49]	DeepRT[11]	26051	1371	3047		HILIC
LUNA HILIC[49]	DeepRT[11]	23512	1237	2750		HILIC
SCX[49]	DeepRT[11]	21638	1138	2530		SCX
Yeast 2h[50]	Custom workflow	15822	832	1850	PXD003472	RP
HeLa lumos 1h[47]	Custom workflow	13310	700	1556	PXD013477	RP
Yeast 1h[50]	Custom workflow	12197	641	1426	PXD003472	RP
Arabidopsis[51]	Custom workflow	10132	533	1185	PXD008812	RP
Yeast DeepRT[52]	DeepRT[11]	4867	256	569		RP
ProteomeTools PTM[41]	Custom workflow ProteomeTools PTM	3659	192	428	PXD009449	RP
Plasma lumos 2h[47]	Custom workflow	2997	157	350	PXD013477	RP
HeLa DeepRT[53]	DeepRT[11]	2917	153	341		RP

637

638

639 Supplemental Table 3: Peptide used to calibrate retention time in the *Custom workflow ProteomeTools*

Calibration peptides
TFAHTESHISK
ISLGEHEGGGK
LSSGYDGTSYK
LYSYYSSTESK
GFLDYESTGAK
HDTVFGSYLYK
ASDLLSGYYIK
GFVIDDGLITK
GASDFLSFAVK

640

641 Supplemental Table 4: Peptide used to calibrate retention time in the *Custom workflow ProteomeTools PTM*

Calibration peptides
TFAHTESHISK
HLTGLTFDTYK
YGFSSEDIFTK
LYSYYSSTESK
GFLDYESTGAK
LSSGYDGTSYK
FLFTGYDTSVK
YFGYTSDTFGK
FLASSEGGFTK
TFTGTTDSFFK
SYASDFGSSAK
HDTVFGSYLYK

642

643